

# FRoundation: Are Foundation Models Ready for Face Recognition?

Tahar Chettaoui<sup>a</sup>, Naser Damer<sup>a,b</sup>, Fadi Boutros<sup>a</sup>

<sup>a</sup>*Fraunhofer Institute for Computer Graphics Research, Darmstadt, 64283, Germany*

<sup>b</sup>*Department of Computer Science, TU Darmstadt, Darmstadt, 64283, Hessen, Germany*

---

## Abstract

Foundation models are predominantly trained in an unsupervised or self-supervised manner on highly diverse and large-scale datasets, making them broadly applicable to various downstream tasks. In this work, we investigate for the first time whether such models are suitable for the specific domain of face recognition. We further propose and demonstrate the adaptation of these models for face recognition across different levels of data availability. Extensive experiments are conducted on multiple foundation models and datasets of varying scales for training and fine-tuning, with evaluation on a wide range of benchmarks. Our results indicate that, despite their versatility, pre-trained foundation models underperform in face recognition compared to similar architectures trained specifically for this task. However, fine-tuning foundation models yields promising results, often surpassing models trained from scratch when training data is limited. Even with access to large-scale face recognition training datasets, fine-tuned foundation models perform comparably to models trained from scratch, but with lower training computational costs and without relying on the assumption of extensive data availability. Our analysis also explores bias in face recognition, with slightly higher bias observed in some settings when using foundation models.

*Keywords:* Face recognition, Foundation models, Computer vision, Face and gesture analyses, Human analyses, fine-tuning

---

## 1. Introduction

Significant progress has been made in developing foundation models trained on extensive and diverse datasets recently [1, 2, 3]. Once these models are

trained, they can be adapted to a wide array of downstream tasks, providing a versatile basis. Inspired by the success of large language models (LLM) [4, 5, 6, 7, 8], similar large-scale foundation models have been explored for various perception tasks [9, 1, 2, 3]. Often based on the Vision Transformer (ViT) architecture [10], which has been shown to match or exceed the performance of traditional methods in large-scale image classification tasks, visual foundation models are becoming increasingly popular due to their strong generalization capabilities when trained on large datasets. Although foundation models hold considerable promise for a wide range of applications, their adaptation for face recognition (FR) has not been explored in previous research, which drives the motivation for this study.

To explore the potential of foundation models in FR, we evaluate the performance of different versions of two widely used foundation models, namely DINOv2 [1] and CLIP [9]. Although foundation models demonstrate strong generalization capabilities, our experiments show that they perform poorly compared to state-of-the-art (SOTA) FR models [11, 12, 13, 14] on various benchmarks. To enhance their effectiveness for the downstream task of FR, we propose to fine-tune the considered foundation models using low-rank adaptation (LoRA) [15]. LoRA integrates trainable low-rank decomposition matrices into each transformer block while keeping the pre-trained model weights frozen. After fine-tuning on dedicated datasets, the LoRA layers adapt to the downstream task of FR, resulting in a significant increase in performance. For example, the smallest released pretrained models of DINOv2 and CLIP achieve average verification accuracies of 64.70% and 82.64%, respectively. After fine-tuning on Casia-Webface, their accuracies increase to 90.94% and 92.13%, respectively.

In addition to examining the performance of fine-tuned foundation models, we compare them to a ViT trained from scratch on different subset sizes of data. This comparison validates the advantages of using foundation models over training an entire model based on data availability. Finally, we investigate the bias in FR and demonstrate that it tends to be slightly higher when fine-tuning foundation models compared to training from scratch.

## 2. Related Work

Foundation models are defined by a substantial number of trainable parameters and are pre-trained on a large and diverse dataset, enabling them to adapt to a wide range of downstream tasks across various domains [16].

Vision foundation models are commonly structured around the use of ViTs [10] and rely on self-supervised learning (SSL) [17]. SSL is a technique that trains models to learn representations from unlabeled data and is essential for training ViTs, which tend to perform poorly on small datasets [18]. Several high-performing vision foundation models specialized in various tasks have been released in recent years. Building on the success of the Segment Anything Model (SAM) [19], which introduced a foundation model for object segmentation, SAM2 [20] presents a model for real-time, promptable object segmentation in images and videos, achieving state-of-the-art performance. CLIP [9] learns visual concepts from natural language supervision and can be applied to any visual classification by providing the names of the visual categories to be recognized. DINOv2 [1] foundation models generate universal features suitable for both image-level visual tasks, such as image classification and video understanding, as well as pixel-level visual tasks, including depth estimation and semantic segmentation.

Vision foundation models are characterized by their generalization ability due to massive training data, but they tend to show poor performance when applied to domain-specific settings [21]. To adapt them to a downstream task, multiple approaches were considered in the literature for this adaption. An example of that is the AdaptFormer [22] that replaces the MLP block in the transformer encoder with two identical MLP branches, where one mirrors the original network and the other introduces a lightweight module for task-specific fine-tuning, demonstrating significant improvements compared to fully fine-tuned models on downstream tasks. Another example is the ViT-Adapter [23] that proposes a technique to adapt plain ViTs for dense prediction tasks by injecting image-related inductive biases into the ViT and reconstructing fine-grained multi-scale features, yielding SOTA results on COCO test-dev. Another approach is to insert trainable rank decomposition matrices, called LoRA [15] layers, while freezing the pre-trained model weights. In this work, we choose LoRA as our foundation model adapter, as recent studies [24, 25, 26, 27, 21] highlight the significant potential of LoRA for this purpose. For instance, integrating LoRA layers into DINOv2 has been successfully applied in the medical domain for two distinct tasks: capsule endoscopy diagnosis [24] and depth estimation in endoscopic surgery [25], both of which have demonstrated superior performance in their respective fields. In another work on adapting foundation models for multiple plant phenotyping [26], Chen et al. demonstrated that LoRA consistently outperforms decoder tuning in leaf counting and disease classification, with their

method achieving high performance in both tasks, approaching the results of SOTA models. Zanella et al. [27] explored few-shot adaptation of Vision Language Models (VLMs) using LoRA, showing that their CLIP-based method not only achieves substantial improvements but also reduces training times.

The application of foundation models in biometrics is still very limited, with only few recent works started investigating their potential. For example, Iris-SAM [28], which is based on the foundation model SAM [19], fine-tunes it on ocular images for iris segmentation, achieving an average segmentation accuracy that surpasses the best baseline by a substantial margin of 10% on the ND-IRIS-0405 dataset. Arc2Face [29] is an identity-conditioned face foundation model that generates photo-realistic images based on the ArcFace embedding of a person. To showcase the performance of the generated data, they train a FR model on synthetic images from their model, achieving superior performance compared to existing synthetic datasets [30]. Recognizing the immense potential of foundation models across diverse tasks, this study breaks new ground by exploring their adaptation for FR, a path, to the best of our knowledge, unexplored until now.

### 3. Methodology

This section presents our approach FRoundation, for optimizing vision foundation models for FR. This section starts by providing details on the selected baseline foundation models, CLIP [9] and DINOv2 [1]. Then, we provide details on the adaptation mechanism used to optimize foundation models for downstream tasks. Finally, we conclude by describing the extension of pretrained foundation models with LoRA for FR.

#### 3.1. Baseline Foundation Models

We selected two state-of-the-art foundation models, CLIP and DINOv2, to conduct our studies in this paper. These models proved to be generalizable across different downstream tasks [1, 9] and achieved very competitive results with zero-shot learning. Previous works [24, 25] also proved that fine-tuning these models using, for example LoRA, could lead to SOTA performance on specific downstream tasks.

##### 3.1.1. DINOv2

DINOv2 [1] is a self-supervised image encoder trained on a large curated dataset, namely the LVD-142M dataset. The dataset was created as part of

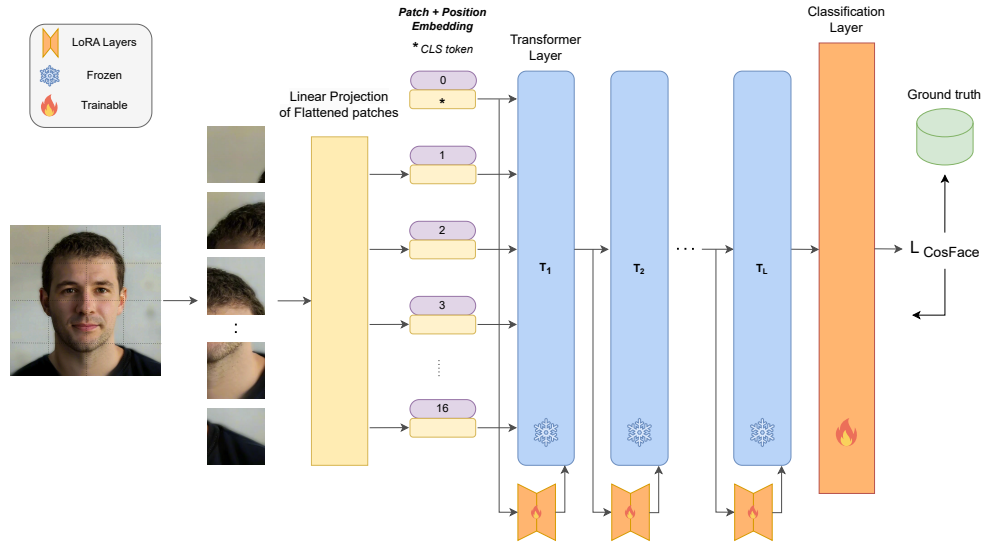


Figure 1: ViT Training Pipeline with LoRA Adapters. The transformer layers remain fixed during training, while trainable LoRA layers are introduced for fine-tuning the model. Each LoRA layer operates independently within the transformer layers and possesses its own set of weights

this initiative, using an automated pipeline to assemble a dedicated, diverse, and curated collection of images. The model network architecture follows a student-teacher framework based on ViT [10] that learns features at the image and patch levels by combining DINO [31] and iBOT [32] losses. The image-level objective, inspired by DINO, is derived from the cross-entropy loss between features extracted from the student and teacher networks. These features are taken from the ViT class token and are based on different crops of the same image. For the patch-level objective, random input patches are masked and sent to the student, while remaining visible to the teacher. The student’s iBOT head processes the masked tokens while the teacher’s iBOT head processes the corresponding visible tokens, leading to the calculation of the loss term. Additionally, several contributions were made to accelerate and stabilize large-scale training. As a result, a ViT model with 1B parameters was trained and distilled into a series of smaller models that surpass the best available general-purpose features on most of the benchmarks at image and pixel levels [1], making it a top candidate as a foundation model for FR.

### 3.1.2. CLIP

Introduced by Radford et al. [9], Contrastive Language-Image Pretraining (CLIP) is a multimodal foundation model that jointly learns from visual and textual modalities. It leverages a large dataset comprising images paired with text description, enabling the model to learn and relate visual information to textual context, and vice versa. The architecture consists of two separate encoders to process image and text inputs, respectively. During training, CLIP employs a contrastive learning approach, maximizing the cosine similarity between feature representations obtained from image-text pairs while minimizing it for negative samples. This allows the model to effectively capture the relationship between images and their corresponding textual descriptions. The training process involves a large-scale training dataset, facilitating the model’s ability to generalize across a variety of visual and textual tasks. In this work, we will focus exclusively on employing the image encoder as we aim to obtain feature representation from face images for the face verification task.

### 3.2. Fine-tuning with LoRA

In this work, we utilized Low-rank adaptation (LoRA) [15] to fine-tune the considered foundation model. LoRA was initially developed to fine-tune LLMs for specific downstream tasks, but it can be applied to any neural network with dense layers. Its development was inspired by [33], which demonstrates that a low-dimensional reparameterization can be as effective for fine-tuning as the full parameter space. This indicates that pre-trained models actually reside on a low intrinsic dimension. Building on this concept, LoRA freezes the pre-trained model weights and inserts trainable rank decomposition matrices into each layer of pretrained transformer architecture. For a pre-trained weight matrix  $W_0 \in \mathbb{R}^{d \times k}$ , LoRA utilizes a low-rank decomposition to restrict its update by  $W_0 + \Delta W = W_0 + BA$  where  $B \in \mathbb{R}^{d \times r}$  and  $A \in \mathbb{R}^{r \times k}$  with the rank  $r \ll \min(d, k)$ .  $W_0$  does not receive gradient updates during the training process, while only  $A$  and  $B$  are updated. When fine-tuning, this approach significantly reduces the number of trainable parameters compared to fine-tuning all model parameters, while also not introducing any additional inference latency. The latter is achieved by computing  $W = W_0 + BA$ . After fine-tuning the model, the adapter weights  $BA$  are merged with the base model weight  $W_0$  to compute the final model weights  $W$ .

During the forward pass, the low-rank matrix product  $BA$  is scaled by  $\frac{\alpha}{r}$  where  $\alpha$  is a constant. When optimizing with Adam [34], tuning  $\alpha$  is roughly the same as tuning the learning rate [15]. This scaling factor causes gradient collapse as the rank increases, resulting in larger ranks performing no better than smaller ones [35]. To tackle this issue, the rank-stabilized LoRA (rsLoRA) [35] method proposes to scale the low-rank matrix with  $\frac{\alpha}{\sqrt{r}}$ . Gradients do not collapse with rsLoRA, and training with higher ranks has been experimentally validated to improve performance. This method allows for an effective compute/performance trade-off, where higher ranks can be used to achieve higher performance at the cost of increased training compute.

### 3.3. FRoundation

Utilizing pretrained foundation model for FR leads to suboptimal results, as will be presented in Section 5.1. Thus, we propose to fine-tune the considered foundation models using LoRA. This requires extending the pretrained ViT models with LoRA layers before fine-tuning them on dedicated datasets. It is possible to apply LoRA to the  $q$ ,  $k$ ,  $v$ , and  $o$  projection layers, which refer respectively to the query, key, value, and output projection matrices in the self-attention module of ViT architecture [10]. Following [15], we adapt the weight matrices of  $q$  and  $v$  only, as it was shown that adapting their respective weights  $W^q$  and  $W^v$  yields the best results on different downstream tasks [15].

The transformer encoder consists of alternating layers of Multiheaded Self-Attention (MSA) and multilayer perceptron (MLP) blocks. Layer Normalization (LN) is applied before every block and residual connections after every block. LoRA is applied exclusively to the attention weights, leaving the MLP unchanged for both simplicity and parameter efficiency [15]. As illustrated in Fig 1, given a facial image, the image is divided into non-overlapping patches which are then mapped into patch embeddings using a linear projection layer. Additionally, a learnable embedding known as the class (CLS) token [10] is appended to the sequence of embedded patches. The goal of the CLS token is to serve as the image representation, which we utilized to obtain feature representation from input face samples. Then, position embeddings are incorporated into the patch embeddings to preserve positional information. The resulting sequence of embedding vectors is used as input for the encoder. In MSA, we run  $k$  heads in parallel, each with its

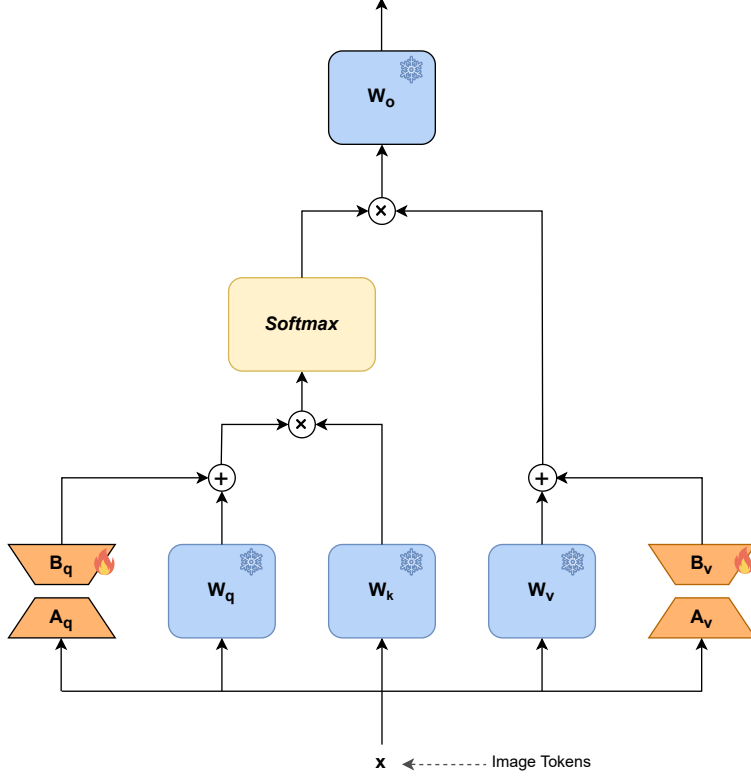


Figure 2: LoRA Integration in Multi-Headed Self-Attention Block. We implement LoRA to  $q$  and  $v$  projection layers in each transformer block.

own set of  $q$ ,  $k$ , and  $v$ . In each head, LoRA layers operate separately and have their own distinct weights. As shown in Fig 2, for an embedding  $x$ , the computation of the  $q$ ,  $k$ , and  $v$  projection layers in head  $i$  are:

$$\begin{aligned}
 Q_i &= W_i^q x + B_i^q A_i^q x, \\
 K_i &= W_i^k x, \\
 V_i &= W_i^v x + B_i^v A_i^v x
 \end{aligned} \tag{1}$$

$W_i^q$ ,  $W_i^k$ , and  $W_i^v$  are frozen projection layers for  $q$ ,  $k$ , and  $v$ , respectively, while  $A_i^q$ ,  $B_i^q$ ,  $A_i^v$ , and  $B_i^v$  are the trainable LoRA layers. Then the attention scores are computed for all heads using a scaled dot-product attention

mechanism. The attention output for head  $i$  is:

$$Attention(Q_i, K_i, V_i) = Softmax\left(\frac{Q_i K_i^T}{\sqrt{d_k}}\right) V_i, \quad (2)$$

where the scaling factor  $d_k$  represents the dimension of the key vectors. The output of all heads is concatenated along the feature dimension and passed through the projection layer  $O$ :

$$MutliHead(Q, K, V) = Concat(head_1, \dots, head_k)W^o. \quad (3)$$

The output of the projection layer  $O$  is then passed to the MLP, completing the execution of a single transformer block.  $L$  transformer layers are used to transform the image tokens into feature representations  $t^l$  where  $l$  denotes the output of the  $l$ -th transformer block. Each  $l$ -th transformer layer processes the output vectors of the previous layer. The final hidden state of the CLS token is employed as feature representation. To optimize the considered foundation models for FR, we proposed to fine-tune the models with the widely adapted margin-penalty softmax loss for FR [12, 11]. Specifically, we extended the architecture with an additional multi-class classification layer and utilized CosFace loss [12] as a margin-penalty softmax loss.

Table 1: The achieved verification performances by DINOv2 and CLIP on several evaluation benchmarks. The results are reported in (%) on the small benchmarks and as average accuracies. The results of the first row are achieved by the ViT-S model trained from scratch on MS1MV2 and provided as a reference. The DINOv2 dataset blurred faces during training, as discussed in Section 5.1, which causes the gap in evaluation accuracies between the two models.

Method	Backbone	LFW	CFPPF	AgeDB30	CALFW	CPLFW	Avg.	LJB-B			LJB-C		
								$10^{-3}$	$10^{-4}$	$10^{-5}$	$10^{-3}$	$10^{-4}$	$10^{-5}$
Baseline (MS1MV2)	ViT-S	99.73	95.44	97.42	95.95	92.35	96.18	95.89	92.85	79.68	96.76	94.51	88.30
DINOv2	ViT-S	78.73	71.15	54.70	59.47	59.48	64.70	14.66	5.90	2.33	18.10	7.44	2.87
	ViT-B	80.22	<b>72.64</b>	56.45	59.77	63.10	66.44	15.13	5.77	2.44	18.21	6.90	2.59
	ViT-L	<b>80.37</b>	71.97	55.25	<b>60.52</b>	<b>64.33</b>	66.49	17.18	6.44	2.52	<b>20.36</b>	7.84	2.77
	ViT-G	80.32	71.97	<b>58.62</b>	59.53	64.20	<b>66.93</b>	<b>17.59</b>	<b>6.76</b>	<b>2.79</b>	19.94	<b>8.05</b>	<b>3.23</b>
CLIP	ViT-B/32	94.03	84.91	70.72	76.13	77.47	80.65	39.36	20.58	9.38	43.73	25.02	11.98
	ViT-B/16	93.33	88.86	74.67	77.13	79.23	82.64	49.19	27.79	11.93	52.21	32.40	16.34
	ViT-L/14	95.90	90.66	<b>79.82</b>	<b>83.10</b>	<b>82.73</b>	<b>86.44</b>	<b>62.72</b>	<b>40.90</b>	<b>20.52</b>	<b>64.74</b>	<b>44.69</b>	<b>25.23</b>
	ViT-L/14@336	<b>96.30</b>	<b>91.26</b>	79.80	81.83	82.30	86.30	61.88	39.69	18.86	64.30	43.68	24.13

## 4. Experimental setups

*Evaluation Datasets.* To explore the capabilities of foundation models for FR, we assess their performance using the following benchmarks: Labeled

Faces in the Wild (LFW) [36], Celebrities in Frontal-Profile in the Wild (CFP-FP) [37], AgeDB30 [38], Cross-age LFW (CA-LFW) [39], CrossPose LFW (CP-LFW) [40]. The results are reported on each benchmark as verification accuracies in (%) and following their official evaluation protocol. In addition, we evaluated on large-scale evaluation benchmarks, IARPA Janus Benchmark-B (IJB-B) [41], and IARPA Janus Benchmark-C (IJB-C) [42]. For IJB-C and IJB-B, we used the official 1:1 mixed verification protocol and reported the verification performance as true acceptance rates (TAR) at false acceptance rates (FAR) of 1e-3, 1e-4, and 1e-5. All these benchmarks were chosen as they are widely used to benchmark the latest FR developments and provide a comprehensive variation of use-cases [11, 12, 13, 14].

*Training and Fine-tuning Datasets.* To fine-tune the considered foundation models, we employ the CASIA WebFace [43] dataset, consisting of 0.5 million images and 10k identities. We also conduct large-scale fine-tuning on the MS1MV2 [11] and WebFace4M [44] datasets. MS1MV2 is a refined version of MS-Celeb-1M [45] by [11], containing 5.8M images of 85K identities. WebFace4M is a subset of the WebFace260M dataset [44], consisting of 200k identities and 4 million images. The images in the training and testing dataset are aligned and cropped to  $112 \times 112$  as described in [11] using five landmark points extracted by the Multi-task Cascaded Convolutional Networks (MTCNN) [46].

*Model architectures.* DINOv2 [1] officially released four ViT architectures, small (ViT-S), base (ViT-B), large (ViT-L), and giant (ViT-G). ViT-S, ViT-B, ViT-L and ViT-G contain 21M, 86M, 0.3B and 1.1B parameters, respectively. All models use a patch size of 14, but they differ in embedding dimensions and the number of attention heads. On the other hand, CLIP [9] offers 4 different models with 2 architectures: base and large. The base model ViT-B of CLIP contains 86M parameters and has 2 variants with different patch sizes, 16 and 32. The large model ViT-L/14 has 0.3 billion parameters and includes a variant that was pre-trained at a higher resolution of 336 pixels for one additional epoch to boost performance [47]. We will start by evaluating the performance of all models in Section 5.1. For further detailed experiments, we focus on the following models: ViT-S for DINOv2 and ViT-B for CLIP, as these are the smallest models released by the corresponding authors, which makes our detailed experiments viable (given hardware and time limitations). We also investigate the performance of the larger models

in Section 5.2 and choose ViT-L for CLIP and DINOv2 for a fairer comparison, as the largest model, namely the giant model of DINOv2, has 1.1 billion parameters compared to 0.3 billion parameters for DINOv2 and CLIP ViT Large.

*Training Settings.* We utilize the CosFace [12] loss function to train all the presented models in this paper with a margin penalty of 0.3 and scale factor of 64, following [12], as well as other works analyzing different building blocks of FR [48]. During the fine-tuning, we used AdamW [49] optimizer with a weight decay of 0.05. We train for 40 epochs (on CaisaWebFace) and for 30 epochs (on MS1MV2 and WebFace4M), with a batch size set to 512 [11]. The initial learning rate is set to 0.0001 and is updated using a Cosine Learning Rate scheduler [50]. Additionally, the LoRA rank is set to 16 for all applicable experiments. The images are resized to  $224 \times 224$  pixels to adapt to the image resolution initially used by DINOv2 and CLIP during training. For data augmentation, we apply horizontal flipping and RandAug [51] with a number of 4 operations and a magnitude of 16, following [52]. We additionally trained 12 instances of ViT, ViT-S and ViT-L, from scratch on different subsets of CASIA-WebFace as well as on MS1MV2 and WebFace4M. These models are noted as Baseline.

## 5. Results

### 5.1. Are Foundation Models ready for Face Recognition?

We first evaluate the face verification performances of the considered foundation models, DINOv2 and CLIP, on the several challenging benchmarks described in Section 4. For DINOv2 and CLIP, we utilized the official pre-trained models released by the corresponding authors [1, 9]. The models, in this case, are utilized as feature extractors without fine-tuning the model weights.

The achieved results by the different pretrained architectures of DINOv2 and CLIP are presented in Table 1. All network architectures are based on vision-transformer (ViT). For details on network architectures, one can refer to the corresponding papers [1, 9]. The results of the first row (noted as Baseline (MS1MV2)) are achieved by a ViT-S model trained from scratch on MS1MV2. These evaluation results are provided in this table as a reference. One can clearly observe that different pretrained CLIP model versions outperformed DINOv2 models on the considered benchmarks. This result

Table 2: The achieved verification performances by baseline model (trained from scratch) and finetune DINOv2 and CLIP on different subsets from CASIA-WebFace. The results are reported in (%) on the small benchmarks and as average accuracies. On IJB-B and IJB-C, the results are reported as TAR at FAR of 1e-3, 1e-4 and 1e-5. The results of the first two rows are obtained from DINOv2 and CLIP models without finetuning. Noting that finetuning DINOv2 and CLIP achieved higher recognition accuracies than training ViT models from scratch on different subsets from CASIA-WebFace.

# Identities	# Images	Method	LFW	CFPPP	AgeDB30	CALFW	CPLFW	Avg.	IJB-B			IJB-C		
									10 <sup>-3</sup>	10 <sup>-4</sup>	10 <sup>-5</sup>	10 <sup>-3</sup>	10 <sup>-4</sup>	10 <sup>-5</sup>
-	-	DINOv2	78.73	71.15	54.70	59.47	59.48	64.70	14.66	5.90	2.33	18.10	7.44	2.87
-	-	CLIP	93.33	88.86	74.67	77.13	79.23	82.64	49.19	27.79	11.93	52.21	32.40	16.34
1k	82425	Baseline	88.33	65.21	61.07	73.35	61.85	69.96	2.44	0.93	0.54	2.69	1.08	0.55
		DINOv2	96.82	87.31	82.20	85.92	83.27	87.10	65.87	45.28	25.54	70.82	51.32	32.66
		CLIP	98.55	93.11	85.28	88.98	87.83	90.75	70.56	43.43	16.36	75.70	51.01	24.86
2k5	163945	Baseline	93.17	74.70	69.93	78.32	71.13	77.45	5.38	1.23	0.51	5.04	1.12	0.41
		DINOv2	97.80	89.60	84.25	87.72	85.15	88.90	72.21	52.88	25.12	77.05	59.88	37.23
		CLIP	98.87	93.51	86.12	90.07	88.78	91.47	71.03	44.12	18.42	76.38	52.58	26.97
2k5 (S)	289228	Baseline	95.78	82.89	78.33	83.25	77.72	83.59	30.37	4.81	1.00	26.91	4.04	0.83
		DINOv2	98.50	90.81	87.25	88.68	85.93	90.23	77.28	61.69	38.96	80.68	66.97	49.67
		CLIP	98.63	94.23	86.28	89.50	88.20	91.37	72.16	41.36	13.18	77.46	51.09	20.48
5k	280215	Baseline	96.32	81.71	78.25	84.23	78.25	83.75	28.63	5.91	1.11	24.17	4.79	1.00
		DINOv2	98.43	90.81	86.83	89.17	85.55	90.16	76.58	61.34	38.03	80.81	66.96	48.81
		CLIP	99.13	94.27	86.85	90.50	88.87	91.92	75.65	53.65	26.92	80.25	59.21	35.83
7k5	389007	Baseline	97.07	85.71	81.55	86.20	81.55	86.42	56.90	18.05	3.03	55.15	17.40	3.80
		DINOv2	98.40	91.94	87.20	89.63	85.60	90.55	74.36	46.42	15.00	77.96	52.97	22.29
		CLIP	99.13	94.49	87.33	90.43	88.45	91.97	77.92	56.26	25.84	81.77	62.78	34.74
10k	490623	Baseline	98.02	88.04	84.70	88.25	83.78	88.56	73.00	39.61	10.48	73.03	36.77	10.79
		DINOv2	98.38	91.57	88.22	89.87	86.67	90.94	79.27	63.24	34.63	82.46	69.50	48.45
		CLIP	98.97	94.29	87.62	90.62	89.13	92.13	80.50	61.45	33.48	83.96	67.45	42.45

might be attributed to the fact that the curated dataset LVD-142M [1], on which DINOv2 was trained, involved a post-processing step that blurred identifiable faces [1]. Although the considered foundation models are not trained and optimized to perform feature extraction for face verification, they achieved relatively high accuracies on considered benchmarks. For example, the achieved verification accuracies by CLIP (ViT-L/14@336), the largest model from CLIP, was 96.30% on LFW. On benchmarks with cross-age evaluation protocol, the best-achieved accuracies on AgeDB30 and CALFW were 79.80% and 81.83%, respectively. All considered models achieved relatively low TAR at the reported thresholds of FAR on large and challenging benchmarks, IJB-B and IJB-C.

From the reported results in Table 1, one can conclude that the achieved results by foundation models on face verification are far from being random. They achieved relatively high accuracies on less challenging benchmarks (LFW). However, this performance significantly drops when the evaluation benchmark contains challenging pairs such as AgeDB30, CALFW, IJB-B and IJB-C, especially when considering the baseline model trained

from scratch and the current performances of state-of-the-art FR solutions [11, 12, 13, 14].

### 5.2. FRoundation: Fine-tuning Foundation Models

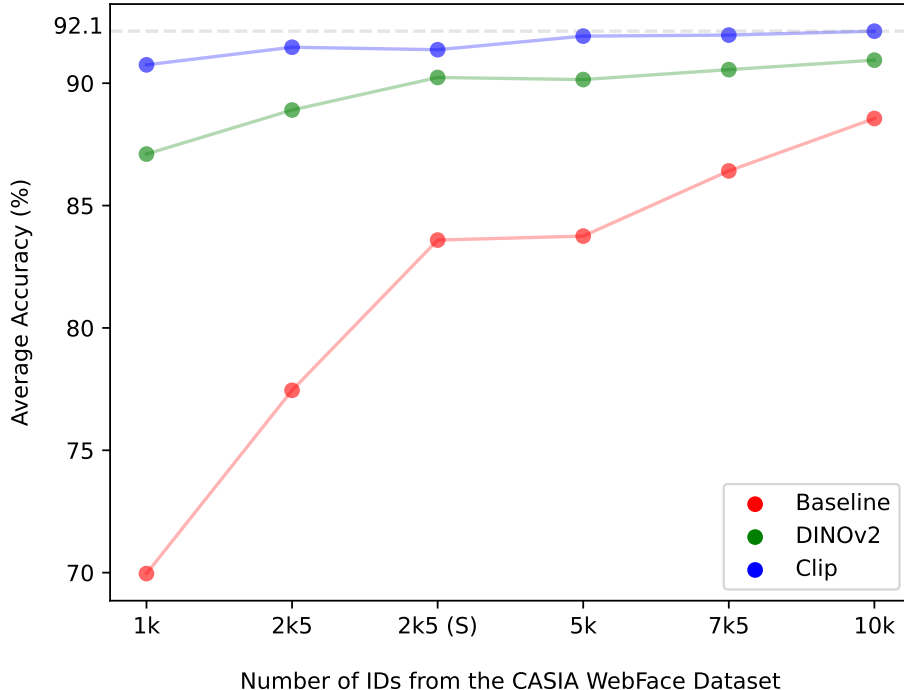


Figure 3: Average verification accuracies on five benchmarks, LFW, CFPFP, AgeDB30, CALFW, CPLFW on the y-axis vs. training/finetuning dataset size, in terms of the number of identities, on the x-axis. The results correspond to the ones reported in Table 2 and plotted for ViT (Baseline) as well as fine-tuned DINOv2 and CLIP. Increasing the training/finetuning dataset width (number of identities) improved the model recognition performances.

Table 2 presents the verification accuracies achieved by considered foundation models, DINOv2 and CLIP, fine-tuned with LoRA (Section 3.3) on different subsets of CASIA-WebFace. The results noted with baseline are achieved by ViT-S trained from scratch and provided as a reference. In this experiment, we utilized the smallest released pretrained ViT architecture from DINOv2 (ViT-S) and CLIP (ViT-B). The results of the first two rows in Table 2 are achieved by pretrained DINOv2 (ViT-S) and CLIP (ViT-B) without finetuning. Driven by possible technical limitations and

ethical concerns in practice to collect large-scale face (or other biometric) datasets [30], we propose to fine-tune the foundation models on small subsets from CAISA-WebFace and compare them to the case where the model was trained from scratch. Specifically, we provided a border evaluation of the impact of dataset size in terms of number of identities (dataset width) on the model performance by utilizing (n)K identities from CAISA-WebFace, where  $n \in [1, 2.5, 5, 7.5, 10]$ . Additionally, we investigate the impact of the dataset depth (number of images) on the model performance by comparing the case where the 2.5k identities are randomly selected to the case where these 2.5K identities are selected (noted as 2.5k (S)) with the largest number of images per identity. The 2.5K and 2.5k (S) resulted in a total of 163945 and 289228 images, respectively. Based on the reported results in Table 2, we made the following observations:

- Fine-tuning DINOv2 and CLIP on different subsets from CASIA-WebFace significantly improved the achieved verification accuracies on all evaluation benchmarks, in comparison to the case where DINOv2 and CLIP are utilized without fine-tuning. Initially, without fine-tuning, DINOv2 (ViT-S) and CLIP (ViT-B) achieved average accuracies of 64.70 and 82.64, respectively. These average accuracies increased to 87.10 and 90.75 by fine-tuning DINOv2 and CLIP, respectively on a small subset of only 1k identities from CAISA-WebFace.
- As expected, using a larger subset for fine-tuning DINOv2 and CLIP consistently resulted in higher verification accuracies across all considered benchmarks. The same observation can be also made for the model trained from scratch (Baseline).
- Finetuning ViT of pretrained DINOv2 and CLIP led to higher verification accuracies, in comparison to the case where the model is trained from scratch. The superiority of foundation models over the model trained from scratch on CASIA-WebFace (or a subset of CASIA-WebFace) can be observed on the small evaluation benchmarks and on the large-scale, IJB-B and IJB-C, benchmarks. This observation can be seen also in Figure 3.
- Figure 3 presents average accuracies (y-axis) of baseline and foundation models fine-tuned on different subsets (x-axis) from CASIA-WebFace. One can notice that the average accuracies slightly improved when

a larger subset of CASIA-WebFace is utilized. On the other hand, the performance of the baseline significantly increases with more data, starting at an average accuracy of 69.96% when trained on 1K and reaching 88.56% on the full dataset with an increase of 18.6%. The same observation can be also made on IJB-B and IJB-C benchmarks (Table 2).

- The impact of the dataset depth (number of images) can be observed by comparing the achieved results of models trained/finetuned on 2.5K (163945) and 2.5K (S) (289228). One can notice that increasing the dataset depth leads to higher verification accuracies in most of the settings.

### 5.3. Large-scale Fine-tuning

Table 3 presented the achieved recognition performances by models trained from scratch (baseline) and fine-tuned (CLIP and DINOv2) on a relatively small dataset, CASIA-WebFace (0.5m images) and larger datasets, MS1MV2 (5.8m images) and WebFace4M (4m images). All results are reported using large (ViT-L) and small (ViT-S of DINOv2 and baseline and ViT-B of CLIP) architectures. We made the following observation from the reported results in Table 3:

- Using CASIA-WebFace (0.5m images), finetuning DINOv2 (ViT-S and ViT-L architectures) and CLIP (ViT-B and ViT-L architectures) led to higher verification accuracies, in comparison to the case where ViT-S and ViT-L are trained from scratch on the same data. For example, the average verification accuracies on the small benchmarks, LFW, CFPFP, AgeDB30, CALFW, and CPLFW, was 87.39% by baseline (ViT-L) which is lower than 94.28% and 94.26% achieved by the fine tuned DINOv2 and CLIP, respectively.
- The models that are trained/finetuned on large datasets, MS1MV2 (5.8m images) and WebFace4M (4m images), achieved higher verification accuracies than the one trained on the relatively smaller dataset, CASIA-WebFace (0.5m images).
- Using small architectures (ViT-S and ViT-B) and large-scale training datasets (MS1MV2 or WebFace4M), the model trained from scratch achieved higher verification accuracies than the finetuned DINOv2 and

CLIP. This observation can be noticed from the achieved results on small benchmarks as well as on large-scale, IJB-B and IJB-C, benchmarks.

- Using large architectures (ViT-L) and large-scale training/finetuning datasets (MS1MV2 or WebFace4M), the finetuned DINOv2 and CLIP achieved slightly higher recognition performance than the models trained from scratch on most of the evaluation benchmarks.

To conclude, for the case where only a relatively small training dataset is accessible, finetuning pretrained foundation models can achieve higher recognition accuracy than training the same model architecture from scratch. In the case that one has access to large training datasets, training a model from scratch for FR can achieve very competitive results to finetuning foundation models. However, this, next to the technical and legal limitations of collecting or maintaining the data, comes with a high training time cost. For example, training ViT-L from scratch on MS1MV2 using the settings described in Section 4 requires around 70 GPU hours on MS1MV2, in comparison to around 40 GPU hours for finetuning DINOv2 with LoRA on 8 Nvidia A100 SXM4 40 GB GPUs.

Table 3: The achieved verification accuracies by baseline models as well as fine-tuned DINOv2 and CLIP on several challenging benchmarks. Different architectures of DINOv2 and CLIP are fine-tuned on different datasets, CASIA-WebFace, MS1MV2 and WebFace4M. The results of baseline refer to model trained from scratch.

Method	Backbone	Train data	LFW	CFPPF	AgeDB30	CALFW	CPLFW	Avg.	IJB-B			IJB-C		
									$10^{-3}$	$10^{-4}$	$10^{-5}$	$10^{-3}$	$10^{-4}$	$10^{-5}$
Baseline	ViT-S	CASIA-WebFace	98.02	88.04	84.70	88.25	83.78	88.56	73.00	39.61	10.48	73.03	36.77	10.79
		MS1MV2	99.73	95.44	97.42	95.95	92.35	96.18	95.89	92.85	79.68	96.76	94.51	88.30
		WebFace4M	99.63	96.57	96.20	95.55	92.92	96.17	96.34	93.86	88.30	97.44	95.62	92.46
	ViT-L	CASIA-WebFace	97.87	87.84	81.53	87.03	82.67	87.39	76.45	58.96	37.88	79.26	62.51	43.95
		MS1MV2	99.73	95.31	96.48	95.68	92.22	95.88	94.76	90.07	74.38	95.85	92.49	82.71
		WebFace4M	99.68	96.47	94.60	94.85	92.63	95.65	95.82	92.92	85.94	97.14	94.79	90.90
DINOv2	ViT-S	CASIA-WebFace	98.38	91.57	88.22	89.87	86.67	90.94	79.27	63.24	34.63	82.46	69.50	48.45
		MS1MV2	99.02	89.71	91.42	92.90	86.83	91.98	89.52	81.70	69.10	91.61	85.25	76.95
		WebFace4M	98.95	91.43	87.77	91.43	87.73	91.46	89.71	81.13	68.34	92.08	85.13	76.10
	ViT-L	CASIA-WebFace	99.33	95.77	92.77	92.33	91.20	94.28	89.98	78.81	61.77	92.44	84.45	72.91
		MS1MV2	99.63	95.93	96.22	95.50	92.78	96.01	95.31	91.95	83.50	96.41	93.94	89.89
		WebFace4M	99.65	96.84	95.10	94.80	93.75	96.03	95.64	92.65	86.42	96.96	94.79	91.40
CLIP	ViT-B	CASIA-WebFace	98.97	94.29	87.62	90.62	89.13	92.13	80.50	61.45	33.48	83.96	67.45	42.45
		MS1MV2	99.43	93.51	92.02	93.37	90.40	93.75	90.82	82.39	65.17	92.82	86.31	75.32
		WebFace4M	99.30	93.93	88.90	92.75	90.67	93.11	90.71	81.52	68.05	92.85	85.63	75.73
	ViT-L	CASIA-WebFace	99.55	95.73	91.73	92.58	91.70	94.26	90.33	78.71	56.96	92.59	83.12	68.87
		MS1MV2	99.68	96.76	93.20	94.60	93.73	95.59	95.73	91.22	82.78	96.80	93.66	88.62
		WebFace4M	99.65	96.50	93.72	94.37	93.73	95.59	95.12	90.72	82.76	96.62	93.40	88.55

#### 5.4. Bias evaluations foundation models FR

We evaluated the baseline model, CLIP and DINOv2 on the Racial Face in the Wild (RFW) dataset [53] to assess the model’s bias and their performance across different demographic groups. The RFW dataset contains four testing subsets corresponding to Caucasian, Asian, Indian, and African demographic groups. Following [54, 53], we reported the results as verification accuracies in (%) on each subset and as average accuracies to evaluate general recognition performance. To evaluate the bias, we reported the standard deviation (STD) between all subsets and the skewed error ratio (SER), which is given by  $\frac{\max_g \text{Error}_g}{\min_g \text{Error}_g}$ ,  $g$  is the demographic group, as reported in [54, 55]. A higher STD value indicates more bias across demographic groups and vice versa. For SER, the model that achieved a value closer to 1 is less biased. Table 4 presents the evaluation results on RFW. As baseline models, we reported the results for ViT-S and ViT-L (noted as Baseline) trained from scratch on CAISA-WebFace, MS1MV2, and WebFace4M. We also reported the results of DINOv2 and CLIP without finetuning and for the case where the models are finetuned on CAISA-WebFace, MS1MV2 or WebFace4M. One can observe the following from the reported results in Table 4:

- Finetuning DINOv2 and CLIP improved the general recognition performance on all demographics, in comparison to the case where pretrained DINOv2 and CLIP are used without finetuning. These results are complementary to the ones reported in the previous section.
- In general, all models achieved their best recognition performances on the Caucasian subset and, in most of the settings, the lowest recognition performances on the African subset.
- Using CASIA-WebFace (0.5m images) for training/finetuning, the finetuned DINOv2 and CLIP achieved higher recognition performances than the model trained from scratch. However, DINOv2 and CLIP are slightly more biased than baseline models. For example, the STD achieved by baseline (ViT-S) was 4.38, which is slightly lower than the 4.49 and 4.43 STD achieved by finetuned DINOv2 (ViT-S) and CLIP (ViT-B).
- The models trained from scratch on large-scale datasets, MS1MV2 (5.8M images) and WebFace4M (4m images) archived higher average recognition performances (average) and lower standard deviation (in

most of the settings) than finetuned CLIP and DINOv2. For example, using ViT-L architecture trained/finetuned on WebFace4M, the baseline achieved an average accuracy of 93.80%, in comparison to 93.43% and 91.57% achieved by DINOv2 and CLIP, respectively. Also, in this case, the baseline model achieved a lower STD (1.74) than DINOv2 (1.78) and CLIP (2.11).

- In general, finetuned DINOv2 achieved higher average accuracies and lower STD than finetuned CLIP.
- Finetuning larger model architectures of pretrained DINOv2 (ViT-L) or CLIP (ViT-L) achieved higher recognition accuracies and lower STD than finetuning smaller architectures, DINOv2 (ViT-S) or CLIP (ViT-B).

Table 4: Evaluation results on RFW reported as average recognition performance in (%), standard deviation (STD) and skewed error ratio (SER) across four different demographic groups. The higher STD indicates a more biased model and the higher average (avg) indicates, in general, better recognition performance.

Method	Backbone	Train data	African	Asian	Caucasian	Indian	Avg.	STD	SER
Baseline	ViT-S	CASIA-WebFace	75.25	75.68	84.75	78.58	78.57	4.38	1.62
		MS1MV2	96.65	96.32	98.63	96.68	97.07	1.05	2.68
		WebFace4M	94.40	94.12	97.73	95.02	95.32	1.65	2.59
	ViT-L	CASIA-WebFace	71.87	73.47	81.08	74.23	75.16	4.06	1.48
		MS1MV2	97.32	96.48	98.45	97.25	97.38	0.81	2.27
		WebFace4M	93.37	92.25	96.33	93.27	93.80	1.75	2.11
DINOv2	ViT-S	-	54.77	61.13	65.00	60.42	60.33	4.21	1.29
		CASIA-WebFace	76.15	76.90	85.98	80.65	79.92	4.49	1.70
		MS1MV2	83.43	83.77	91.18	87.05	86.36	3.60	1.87
	ViT-L	WebFace4M	80.83	82.90	88.50	84.77	84.25	3.25	1.66
		-	58.46	64.20	67.47	60.93	62.77	3.91	1.27
		CASIA-WebFace	85.97	84.00	93.15	86.65	87.44	3.96	2.33
CLIP	ViT-B	MS1MV2	93.75	93.40	97.08	93.92	94.54	1.70	2.26
		WebFace4M	92.85	91.75	95.97	93.40	93.49	1.78	2.04
		-	70.75	69.73	79.32	68.98	72.19	4.80	1.49
	ViT-L	CASIA-WebFace	80.13	80.53	89.18	80.30	82.54	4.43	1.83
		MS1MV2	85.60	86.30	91.82	87.40	87.78	2.79	1.76
		WebFace4M	84.43	84.62	90.80	85.97	86.45	2.97	1.69
ViT-L	-	74.03	72.15	82.60	73.15	75.48	4.80	1.60	
	CASIA-WebFace	84.65	84.47	92.60	85.02	86.69	3.94	2.09	
	MS1MV2	90.63	90.77	95.03	91.92	92.09	2.04	1.88	
		WebFace4M	90.40	90.28	94.73	90.90	91.57	2.11	1.84

## 6. Conclusion

This paper was the first to propose and investigate the use of foundation models for the task of FR. We additionally propose the adaption of the foundation models to this specific task under various levels of data availability. Our experiments on multiple foundation models, training datasets, and a wide range set of evaluation benchmarks led to interesting conclusions summarized in the following. The studied pretrained foundation models, used as feature extractors without fine-tuning, demonstrated relatively acceptable (far from random) accuracy on less challenging face verification benchmarks like LFW. However, they under-performed on more challenging benchmarks such as AgeDB30, CALFW, IJB-B, and IJB-C. Our adaption of foundation models to FR showed that fine-tuning these models on even small subsets of CASIA-WebFace, e.g. 1k identities, significantly boosts their verification accuracy across benchmarks, outperforming models trained from scratch on similar data subsets. Additionally, increasing the dataset size (dataset width) or the number of images per identity (dataset depth) enhances performance, demonstrating the scalability of foundation models with diverse data availability. The results additionally showed that, with a limited training dataset like CASIA-WebFace, fine-tuning pretrained foundation models outperforms training models from scratch in recognition accuracy. However, when large datasets (MS1MV2 or WebFace4M) are available, training from scratch yields competitive performance, though it incurs a significantly higher training computational cost compared to fine-tuning. Our bias evaluation results indicate that fine-tuning foundation models enhance recognition performance across demographics but introduces slightly more bias compared to baseline models trained from scratch, especially on smaller fine-tuning datasets. Models trained from scratch on larger datasets (MS1MV2 and WebFace4M) achieved superior recognition accuracy and exhibited lower bias. The outcomes of this work set the stage for broader adoption of foundation models as a basis for biometric recognition, particularly in scenarios with limited data availability, being aware of the technical and legal constraints on biometric data collection and management.

## Acknowledgments

This research work has been funded by the German Federal Ministry of Education and Research and the Hessen State Ministry for Higher Education,

Research and the Arts within their joint support of the National Research Center for Applied Cybersecurity ATHENE.

## References

- [1] M. Oquab, T. Darcet, T. Moutakanni, H. Vo, M. Szafraniec, V. Khaldov, P. Fernandez, D. Haziza, F. Massa, A. El-Nouby, M. Assran, N. Ballas, W. Galuba, R. Howes, P.-Y. Huang, S.-W. Li, I. Misra, M. Rabbat, V. Sharma, G. Synnaeve, H. Xu, H. Jegou, J. Mairal, P. Labatut, A. Joulin, P. Bojanowski, Dinov2: Learning robust visual features without supervision, 2024. URL: <https://arxiv.org/abs/2304.07193>. arXiv:2304.07193.
- [2] H. Bao, L. Dong, S. Piao, F. Wei, Beit: Bert pre-training of image transformers, 2022. URL: <https://arxiv.org/abs/2106.08254>. arXiv:2106.08254.
- [3] K. He, X. Chen, S. Xie, Y. Li, P. Dollár, R. Girshick, Masked autoencoders are scalable vision learners, 2021. URL: <https://arxiv.org/abs/2111.06377>. arXiv:2111.06377.
- [4] J. Devlin, M.-W. Chang, K. Lee, K. Toutanova, Bert: Pre-training of deep bidirectional transformers for language understanding, 2019. URL: <https://arxiv.org/abs/1810.04805>. arXiv:1810.04805.
- [5] T. B. Brown, B. Mann, N. Ryder, M. Subbiah, J. Kaplan, P. Dhariwal, A. Neelakantan, P. Shyam, G. Sastry, A. Askell, S. Agarwal, A. Herbert-Voss, G. Krueger, T. Henighan, R. Child, A. Ramesh, D. M. Ziegler, J. Wu, C. Winter, C. Hesse, M. Chen, E. Sigler, M. Litwin, S. Gray, B. Chess, J. Clark, C. Berner, S. McCandlish, A. Radford, I. Sutskever, D. Amodei, Language models are few-shot learners, 2020. URL: <https://arxiv.org/abs/2005.14165>. arXiv:2005.14165.
- [6] H. Touvron, T. Lavril, G. Izacard, X. Martinet, M.-A. Lachaux, T. Lacroix, B. Rozière, N. Goyal, E. Hambro, F. Azhar, A. Rodriguez, A. Joulin, E. Grave, G. Lample, Llama: Open and efficient foundation language models, 2023. URL: <https://arxiv.org/abs/2302.13971>. arXiv:2302.13971.

- [7] A. Chowdhery, S. Narang, J. Devlin, M. Bosma, G. Mishra, A. Roberts, P. Barham, H. W. Chung, C. Sutton, S. Gehrmann, P. Schuh, K. Shi, S. Tsvyashchenko, J. Maynez, A. Rao, P. Barnes, Y. Tay, N. Shazeer, V. Prabhakaran, E. Reif, N. Du, B. Hutchinson, R. Pope, J. Bradbury, J. Austin, M. Isard, G. Gur-Ari, P. Yin, T. Duke, A. Levskaya, S. Ghemawat, S. Dev, H. Michalewski, X. Garcia, V. Misra, K. Robinson, L. Fedus, D. Zhou, D. Ippolito, D. Luan, H. Lim, B. Zoph, A. Spiridonov, R. Sepassi, D. Dohan, S. Agrawal, M. Omernick, A. M. Dai, T. S. Pillai, M. Pellat, A. Lewkowycz, E. Moreira, R. Child, O. Polozov, K. Lee, Z. Zhou, X. Wang, B. Saeta, M. Diaz, O. Firat, M. Catasta, J. Wei, K. Meier-Hellstern, D. Eck, J. Dean, S. Petrov, N. Fiedel, Palm: Scaling language modeling with pathways, 2022. URL: <https://arxiv.org/abs/2204.02311>. arXiv:2204.02311.
- [8] G. Team, R. Anil, S. Borgeaud, Y. Wu, J.-B. Alayrac, J. Yu, R. Soricut, J. Schalkwyk, A. M. Dai, A. Hauth, al., Gemini: A family of highly capable multimodal models, 2024. URL: <https://arxiv.org/abs/2312.11805>. arXiv:2312.11805.
- [9] A. Radford, J. W. Kim, C. Hallacy, A. Ramesh, G. Goh, S. Agarwal, G. Sastry, A. Askell, P. Mishkin, J. Clark, G. Krueger, I. Sutskever, Learning transferable visual models from natural language supervision, 2021. URL: <https://arxiv.org/abs/2103.00020>. arXiv:2103.00020.
- [10] A. Dosovitskiy, L. Beyer, A. Kolesnikov, D. Weissenborn, X. Zhai, T. Unterthiner, M. Dehghani, M. Minderer, G. Heigold, S. Gelly, J. Uszkoreit, N. Houlsby, An image is worth 16x16 words: Transformers for image recognition at scale, 2021. URL: <https://arxiv.org/abs/2010.11929>. arXiv:2010.11929.
- [11] J. Deng, J. Guo, J. Yang, N. Xue, I. Kotsia, S. Zafeiriou, Arcface: Additive angular margin loss for deep face recognition, *IEEE Transactions on Pattern Analysis and Machine Intelligence* 44 (2022) 5962–5979. URL: <http://dx.doi.org/10.1109/TPAMI.2021.3087709>. doi:10.1109/tpami.2021.3087709.
- [12] H. Wang, Y. Wang, Z. Zhou, X. Ji, D. Gong, J. Zhou, Z. Li, W. Liu, Cosface: Large margin cosine loss for deep face recognition, 2018. URL: <https://arxiv.org/abs/1801.09414>. arXiv:1801.09414.

- [13] F. Boutros, N. Damer, F. Kirchbuchner, A. Kuijper, Elasticface: Elastic margin loss for deep face recognition, in: IEEE/CVF Conference on Computer Vision and Pattern Recognition Workshops, CVPR Workshops 2022, New Orleans, LA, USA, June 19-20, 2022, IEEE, 2022, pp. 1577–1586. URL: <https://doi.org/10.1109/CVPRW56347.2022.00164>. doi:10.1109/CVPRW56347.2022.00164.
- [14] J. Dan, Y. Liu, H. Xie, J. Deng, H. Xie, X. Xie, B. Sun, Transface: Calibrating transformer training for face recognition from a data-centric perspective, in: IEEE/CVF International Conference on Computer Vision, ICCV 2023, Paris, France, October 1-6, 2023, IEEE, 2023, pp. 20585–20596. URL: <https://doi.org/10.1109/ICCV51070.2023.01887>. doi:10.1109/ICCV51070.2023.01887.
- [15] E. J. Hu, Y. Shen, P. Wallis, Z. Allen-Zhu, Y. Li, S. Wang, L. Wang, W. Chen, Lora: Low-rank adaptation of large language models, 2021. URL: <https://arxiv.org/abs/2106.09685>. arXiv:2106.09685.
- [16] R. Bommasani, D. A. Hudson, E. Adeli, R. Altman, S. Arora, S. von Arx, M. S. Bernstein, J. Bohg, A. Bosselut, E. Brunskill, E. Brynjolfsson, S. Buch, D. Card, R. Castellon, N. Chatterji, A. Chen, K. Creel, J. Q. Davis, D. Demszky, C. Donahue, M. Doumbouya, E. Durmus, S. Ermon, J. Etchemendy, K. Ethayarajh, L. Fei-Fei, C. Finn, T. Gale, L. Gillespie, K. Goel, N. Goodman, S. Grossman, N. Guha, T. Hashimoto, P. Henderson, J. Hewitt, D. E. Ho, J. Hong, K. Hsu, J. Huang, T. Icard, S. Jain, D. Jurafsky, P. Kalluri, S. Karamcheti, G. Keeling, F. Khani, O. Khattab, P. W. Koh, M. Krass, R. Krishna, R. Kuditipudi, A. Kumar, F. Ladhak, M. Lee, T. Lee, J. Leskovec, I. Levent, X. L. Li, X. Li, T. Ma, A. Malik, C. D. Manning, S. Mirchandani, E. Mitchell, Z. Muniyikwa, S. Nair, A. Narayan, D. Narayanan, B. Newman, A. Nie, J. C. Niebles, H. Nilforoshan, J. Nyarko, G. Ogut, L. Orr, I. Papadimitriou, J. S. Park, C. Piech, E. Portelance, C. Potts, A. Raghunathan, R. Reich, H. Ren, F. Rong, Y. Roohani, C. Ruiz, J. Ryan, C. Ré, D. Sadigh, S. Sagawa, K. Santhanam, A. Shih, K. Srinivasan, A. Tamkin, R. Taori, A. W. Thomas, F. Tramèr, R. E. Wang, W. Wang, B. Wu, J. Wu, Y. Wu, S. M. Xie, M. Yasunaga, J. You, M. Zaharia, M. Zhang, T. Zhang, X. Zhang, Y. Zhang, L. Zheng, K. Zhou, P. Liang, On the opportunities and risks of foundation models, 2022. URL: <https://arxiv.org/abs/2108.07258>. arXiv:2108.07258.

- [17] J. Gui, T. Chen, J. Zhang, Q. Cao, Z. Sun, H. Luo, D. Tao, A survey on self-supervised learning: Algorithms, applications, and future trends, 2024. URL: <https://arxiv.org/abs/2301.05712>. arXiv:2301.05712.
- [18] H. Zhu, B. Chen, C. Yang, Understanding why vit trains badly on small datasets: An intuitive perspective, 2023. URL: <https://arxiv.org/abs/2302.03751>. arXiv:2302.03751.
- [19] A. Kirillov, E. Mintun, N. Ravi, H. Mao, C. Rolland, L. Gustafson, T. Xiao, S. Whitehead, A. C. Berg, W.-Y. Lo, P. Dollár, R. Girshick, Segment anything, 2023. URL: <https://arxiv.org/abs/2304.02643>. arXiv:2304.02643.
- [20] N. Ravi, V. Gabeur, Y.-T. Hu, R. Hu, C. Ryali, T. Ma, H. Khedr, R. Rädle, C. Rolland, L. Gustafson, E. Mintun, J. Pan, K. V. Alwala, N. Carion, C.-Y. Wu, R. Girshick, P. Dollár, C. Feichtenhofer, Sam 2: Segment anything in images and videos, 2024. URL: <https://arxiv.org/abs/2408.00714>. arXiv:2408.00714.
- [21] A. Wang, M. Islam, M. Xu, Y. Zhang, H. Ren, Sam meets robotic surgery: An empirical study on generalization, robustness and adaptation, 2023. URL: <https://arxiv.org/abs/2308.07156>. arXiv:2308.07156.
- [22] S. Chen, C. Ge, Z. Tong, J. Wang, Y. Song, J. Wang, P. Luo, Adapt-former: Adapting vision transformers for scalable visual recognition, 2022. URL: <https://arxiv.org/abs/2205.13535>. arXiv:2205.13535.
- [23] Z. Chen, Y. Duan, W. Wang, J. He, T. Lu, J. Dai, Y. Qiao, Vision transformer adapter for dense predictions, 2023. URL: <https://arxiv.org/abs/2205.08534>. arXiv:2205.08534.
- [24] B. Zhang, Y. Chen, L. Bai, Y. Zhao, Y. Sun, Y. Yuan, J. Zhang, H. Ren, Learning to adapt foundation model dinov2 for capsule endoscopy diagnosis, 2024. URL: <https://arxiv.org/abs/2406.10508>. arXiv:2406.10508.
- [25] B. Cui, M. Islam, L. Bai, H. Ren, Surgical-dino: Adapter learning of foundation models for depth estimation in endoscopic surgery, 2024. URL: <https://arxiv.org/abs/2401.06013>. arXiv:2401.06013.

- [26] F. Chen, M. V. Giuffrida, S. A. Tsaftaris, Adapting vision foundation models for plant phenotyping, in: Proceedings of the IEEE/CVF International Conference on Computer Vision (ICCV) Workshops, 2023, pp. 604–613.
- [27] M. Zanella, I. B. Ayed, Low-rank few-shot adaptation of vision-language models, 2024. URL: <https://arxiv.org/abs/2405.18541>. arXiv:2405.18541.
- [28] P. Farmanifard, A. Ross, Iris-sam: Iris segmentation using a foundation model, 2024. URL: <https://arxiv.org/abs/2402.06497>. arXiv:2402.06497.
- [29] F. P. Papantoniou, A. Lattas, S. Moschoglou, J. Deng, B. Kainz, S. Zafeiriou, Arc2face: A foundation model for id-consistent human faces, 2024. URL: <https://arxiv.org/abs/2403.11641>. arXiv:2403.11641.
- [30] F. Boutros, V. Struc, J. Fiérrez, N. Damer, Synthetic data for face recognition: Current state and future prospects, *Image Vis. Comput.* 135 (2023) 104688. URL: <https://doi.org/10.1016/j.imavis.2023.104688>. doi:10.1016/J.IMAVIS.2023.104688.
- [31] M. Caron, H. Touvron, I. Misra, H. Jégou, J. Mairal, P. Bojanowski, A. Joulin, Emerging properties in self-supervised vision transformers, 2021. URL: <https://arxiv.org/abs/2104.14294>. arXiv:2104.14294.
- [32] J. Zhou, C. Wei, H. Wang, W. Shen, C. Xie, A. Yuille, T. Kong, ibot: Image bert pre-training with online tokenizer, 2022. URL: <https://arxiv.org/abs/2111.07832>. arXiv:2111.07832.
- [33] A. Aghajanyan, L. Zettlemoyer, S. Gupta, Intrinsic dimensionality explains the effectiveness of language model fine-tuning, 2020. URL: <https://arxiv.org/abs/2012.13255>. arXiv:2012.13255.
- [34] D. P. Kingma, J. Ba, Adam: A method for stochastic optimization, 2017. URL: <https://arxiv.org/abs/1412.6980>. arXiv:1412.6980.
- [35] D. Kalajdzievski, A rank stabilization scaling factor for fine-tuning with lora, 2023. URL: <https://arxiv.org/abs/2312.03732>. arXiv:2312.03732.

- [36] G. B. Huang, M. Mattar, T. Berg, E. Learned-Miller, Labeled Faces in the Wild: A Database for Studying Face Recognition in Unconstrained Environments, in: Workshop on Faces in 'Real-Life' Images: Detection, Alignment, and Recognition, Erik Learned-Miller and Andras Ferencz and Frédéric Jurie, Marseille, France, 2008. URL: <https://inria.hal.science/inria-00321923>.
- [37] S. Sengupta, J. Chen, C. Castillo, V. Patel, R. Chellappa, D. Jacobs, Frontal to profile face verification in the wild, in: 2016 IEEE Winter Conference on Applications of Computer Vision, WACV 2016, 2016 IEEE Winter Conference on Applications of Computer Vision, WACV 2016, Institute of Electrical and Electronics Engineers Inc., 2016. doi:10.1109/WACV.2016.7477558, publisher Copyright: © 2016 IEEE.; IEEE Winter Conference on Applications of Computer Vision, WACV 2016 ; Conference date: 07-03-2016 Through 10-03-2016.
- [38] S. Moschoglou, A. Papaioannou, C. Sagonas, J. Deng, I. Kotsia, S. Zafeiriou, Agedb: the first manually collected, in-the-wild age database, in: Proceedings of the IEEE Conference on Computer Vision and Pattern Recognition Workshop, volume 2, 2017, p. 5.
- [39] T. Zheng, W. Deng, J. Hu, Cross-age LFW: A database for studying cross-age face recognition in unconstrained environments, CoRR abs/1708.08197 (2017). URL: <http://arxiv.org/abs/1708.08197>. arXiv:1708.08197.
- [40] T. Zheng, W. Deng, Cross-pose LFW: A database for studying cross-pose face recognition in unconstrained environments, Technical Report 18-01, Beijing University of Posts and Telecommunications, 2018.
- [41] C. Whitelam, E. Taborsky, A. Blanton, B. Maze, J. Adams, T. Miller, N. Kalka, A. Jain, J. Duncan, K. Allen, J. Cheney, P. Grother, Iarpa janus benchmark-b face dataset, 2017, pp. 592–600. doi:10.1109/CVPRW.2017.87.
- [42] B. Maze, J. C. Adams, J. A. Duncan, N. D. Kalka, T. Miller, C. Otto, A. K. Jain, W. T. Niggel, J. Anderson, J. Cheney, P. Grother, IARPA janus benchmark - C: face dataset and protocol, in: 2018 International

- Conference on Biometrics, ICB 2018, Gold Coast, Australia, February 20-23, 2018, IEEE, 2018, pp. 158–165. URL: <https://doi.org/10.1109/ICB2018.2018.00033>. doi:10.1109/ICB2018.2018.00033.
- [43] D. Yi, Z. Lei, S. Liao, S. Z. Li, Learning face representation from scratch, CoRR abs/1411.7923 (2014). URL: <http://arxiv.org/abs/1411.7923>. arXiv:1411.7923.
- [44] Z. Zhu, G. Huang, J. Deng, Y. Ye, J. Huang, X. Chen, J. Zhu, T. Yang, J. Lu, D. Du, J. Zhou, Webface260m: A benchmark unveiling the power of million-scale deep face recognition, 2021. URL: <https://arxiv.org/abs/2103.04098>. arXiv:2103.04098.
- [45] Y. Guo, L. Zhang, Y. Hu, X. He, J. Gao, Ms-celeb-1m: A dataset and benchmark for large-scale face recognition, in: B. Leibe, J. Matas, N. Sebe, M. Welling (Eds.), Computer Vision - ECCV 2016 - 14th European Conference, Amsterdam, The Netherlands, October 11-14, 2016, Proceedings, Part III, volume 9907 of *Lecture Notes in Computer Science*, Springer, 2016, pp. 87–102. URL: [https://doi.org/10.1007/978-3-319-46487-9\\_6](https://doi.org/10.1007/978-3-319-46487-9_6). doi:10.1007/978-3-319-46487-9\_6.
- [46] K. Zhang, Z. Zhang, Z. Li, Y. Qiao, Joint face detection and alignment using multitask cascaded convolutional networks, *IEEE Signal Processing Letters* 23 (2016) 1499–1503.
- [47] H. Touvron, A. Vedaldi, M. Douze, H. Jégou, Fixing the train-test resolution discrepancy, CoRR abs/1906.06423 (2019). URL: <http://arxiv.org/abs/1906.06423>. arXiv:1906.06423.
- [48] F. Boutros, M. Huber, A. T. Luu, P. Siebke, N. Damer, Sface2: Synthetic-based face recognition with w-space identity-driven sampling, *IEEE Trans. Biom. Behav. Identity Sci.* 6 (2024) 290–303. URL: <https://doi.org/10.1109/TBIOM.2024.3371502>. doi:10.1109/TBIOM.2024.3371502.
- [49] I. Loshchilov, F. Hutter, Decoupled weight decay regularization, 2019. URL: <https://arxiv.org/abs/1711.05101>. arXiv:1711.05101.
- [50] I. Loshchilov, F. Hutter, Sgdr: Stochastic gradient descent with warm restarts, 2017. URL: <https://arxiv.org/abs/1608.03983>. arXiv:1608.03983.

- [51] E. D. Cubuk, B. Zoph, J. Shlens, Q. V. Le, Randaugment: Practical automated data augmentation with a reduced search space, in: 2020 IEEE/CVF Conference on Computer Vision and Pattern Recognition, CVPR Workshops 2020, Seattle, WA, USA, June 14-19, 2020, Computer Vision Foundation / IEEE, 2020, pp. 3008–3017. URL: [https://openaccess.thecvf.com/content\\_CVPRW\\_2020/html/w40/Cubuk\\_Randaugment\\_Practical\\_Automated\\_Data\\_Augmentation\\_With\\_a\\_Reduced\\_Search\\_Space\\_CVPRW\\_2020\\_paper.html](https://openaccess.thecvf.com/content_CVPRW_2020/html/w40/Cubuk_Randaugment_Practical_Automated_Data_Augmentation_With_a_Reduced_Search_Space_CVPRW_2020_paper.html). doi:10.1109/CVPRW50498.2020.00359.
- [52] F. Boutros, M. Klemt, M. Fang, A. Kuijper, N. Damer, Exfacegan: Exploring identity directions in gan’s learned latent space for synthetic identity generation, in: IEEE International Joint Conference on Biometrics, IJCB 2023, Ljubljana, Slovenia, September 25-28, 2023, IEEE, 2023, pp. 1–10. URL: <https://doi.org/10.1109/IJCB57857.2023.10449036>. doi:10.1109/IJCB57857.2023.10449036.
- [53] M. Wang, W. Deng, J. Hu, X. Tao, Y. Huang, Racial faces in the wild: Reducing racial bias by information maximization adaptation network, in: 2019 IEEE/CVF International Conference on Computer Vision, ICCV 2019, Seoul, Korea (South), October 27 - November 2, 2019, IEEE, 2019, pp. 692–702. URL: <https://doi.org/10.1109/ICCV.2019.00078>. doi:10.1109/ICCV.2019.00078.
- [54] M. Wang, Y. Zhang, W. Deng, Meta balanced network for fair face recognition, IEEE Trans. Pattern Anal. Mach. Intell. 44 (2022) 8433–8448. URL: <https://doi.org/10.1109/TPAMI.2021.3103191>. doi:10.1109/TPAMI.2021.3103191.
- [55] M. Wang, W. Deng, Mitigate bias in face recognition using skewness-aware reinforcement learning, CoRR abs/1911.10692 (2019). URL: <http://arxiv.org/abs/1911.10692>. arXiv:1911.10692.